

DOI: 10.1002/adfm.200500603

# Three-Dimensionally Ordered Gold Nanocrystal/Silica Superlattice Thin Films Synthesized via Sol–Gel Self-Assembly\*\*

By Hongyou Fan,\* Adam Wright, John Gabaldon, Adrian Rodriguez, C. Jeffrey Brinker, and Ying-Bing Jiang

Nanocrystals and their ordered arrays hold many important applications in fields such as catalysis, surface-enhanced Raman spectroscopy based sensors, memory storage, and electronic and optical nanodevices. Herein, a simple and general method to synthesize ordered, three-dimensional, transparent gold nanocrystal/silica superlattice thin films by self-assembly of gold nanocrystal micelles with silica or organosilanesquioxane by spin-coating is reported. The self-assembly process is conducted under acidic sol–gel conditions (ca. pH 2), ensuring spin-solution homogeneity and stability and facilitating the formation of ordered and transparent gold nanocrystal/silica films. The monodisperse nanocrystals are organized within inorganic host matrices as a face-centered cubic mesostructure, and characterized by transmission electron spectroscopy and X-ray diffraction.

## 1. Introduction

Nanocrystals (NCs) exhibit unique size-dependent optical, electronic, and chemical properties. The ability to adjust properties by controlling size, shape, composition, crystallinity, and structure has led to a wide range of potential applications for NCs in areas such as optics, electronics, catalysis, magnetic storage, and biological labeling.<sup>[1–6]</sup> Furthermore, NC assembly into 2D and 3D superlattices is of interest for development of “artificial solids” with collective optical and electronic properties that can be further tuned by the NC spacing and arrange-

ment.<sup>[7–11]</sup> To date, there have been three approaches to the fabrication of superlattice solids and thin films. The most commonly used approach involves evaporating a drop of NC organic solution on a solid support (e.g., a transmission electron microscopy (TEM) grid, mica, highly ordered pyrolytic graphite (HOPG), etc.), forming face-centered cubic (fcc), body-centered cubic (bcc), or hexagonal close-packed (hcp) superlattice films.<sup>[2,12–14]</sup> Heath and co-workers reported a method to form 2D hcp superlattice films of silver NCs by Langmuir–Blodgett deposition.<sup>[9]</sup> In a third approach, a homogenous precipitation of superlattice solids was prepared by the slow addition of non-solvents into an NC organic solution.<sup>[15,16]</sup> Over a long aging time, well-shaped crystal superlattice solids with fcc structure were finally obtained. The common problem in these approaches is that the NCs that have been used are alkane-chain stabilized, and are therefore hydrophobic and soluble only in organic solvents. The formation of an ordered NC superlattice is limited to organic solvents, and relies on the van der Waals interactions between interdigitated alkane chains surrounding the NCs. The thermally defined, interdigitated alkane chains result in weak mechanical stability of the superlattice. In such materials, charge transport is conducted through the interdigitated organic media between NCs.<sup>[7–11]</sup> Recent results indicate that it is desirable to incorporate NCs in inorganic thin film matrices such as silica or titania for achieving chemical and mechanical robustness and enhanced device functionality.<sup>[17–19]</sup> Early efforts focused on the encapsulation of metal NCs inside sol–gel matrices by introduction of metal nanoparticles<sup>[20]</sup> or metal precursors followed by either thermal decomposition or reduction.<sup>[21,22]</sup> Recently, mesoporous materials have been used as templates to create hybrid silica materials infiltrated with metal or semiconducting NCs.<sup>[23–27]</sup> There are several disadvantages of the above methods, which include: 1) the NC arrays inside the final materials exhibit a poorly defined or less-ordered structure. This is problematic for fundamental studies of charge transport, where repeatable/reproducible results are required.

[\*] Prof. H. Fan, Prof. C. J. Brinker  
Chemical Synthesis and Nanomaterials Department  
Advanced Materials Laboratory  
Sandia National Laboratories  
1001 University Blvd. SE, Albuquerque, NM 87106 (USA)  
E-mail: hfan@sandia.gov

Prof. H. Fan, A. Wright, J. Gabaldon, A. Rodriguez,  
Prof. C. J. Brinker  
NSF Center for Micro-Engineered Materials  
Department of Chemical and Nuclear Engineering  
University of New Mexico  
Albuquerque, NM 87131 (USA)

Dr. Y.-B. Jiang  
Earth and Planetary Sciences  
University of New Mexico  
Albuquerque, NM 87131 (USA)

[\*\*] This work was partially supported by the U.S. Department of Energy (DOE) Basic Energy Sciences Program, Sandia National Laboratory's Laboratory Directed R&D program, the Air Force Office of Scientific Research, and Center for Integrated Nanotechnologies (CINT). We acknowledge use of the SEM facility at University of New Mexico supported by the NSF EPSCOR and NNIN grants. TEM investigations were performed in the Department of Earth and Planetary Sciences at the University of New Mexico. Sandia is a multiprogram laboratory operated by Sandia Corporation, a Lockheed Martin Company, for the United States Department of Energy's National Nuclear Security Administration under Contract DE-AC04-94AL85000.

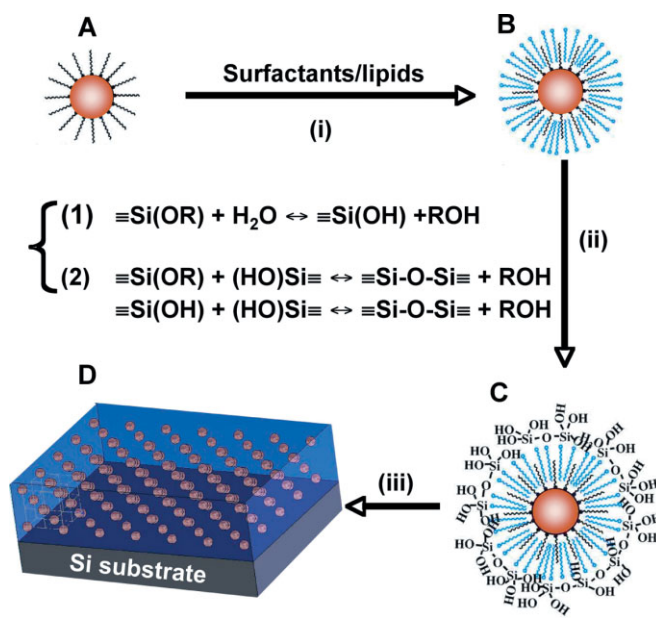
2) The methods have less control over particle sizes and loading. 3) It is difficult to control the interparticle spacing precisely using these methods, and that is essential for achieving new physical properties resulting from coupling between neighboring nanoparticles.<sup>[9,11,28]</sup>

We recently reported a facile synthesis of water-soluble NC micelles<sup>[29–31]</sup> and their self-assembly into ordered, 3D gold-NC/silica superlattice arrays in a sol-gel process.<sup>[19]</sup> Under basic conditions, fast silica hydrolysis and condensation led to a heterogeneous self-assembly system and ordered arrays in solid/powder form.<sup>[19]</sup> For device fabrication, thin films are more desirable than powder. Herein, we report a detailed synthesis of gold-NC/silica arrays in thin film form by a slow sol-gel process under acidic conditions. We discovered that silica condensation played an important role in the formation of ordered 3D gold-NC/silica arrays. It is essential that the coating solution be homogeneous to form ordered, transparent gold/silica thin films without cracking. Extensive silica condensation leads to a less-ordered gold/silica mesophase. To this end, the precursor solution was prepared under acidic conditions (ca. pH 2), using the addition of aqueous hydrogen chloride, to maximize the silica gel time and facilitate the self-assembly and formation of ordered NC/silica thin films.<sup>[32,33]</sup> By using organosilsesquioxane, we were able to tune the framework chemistry and dielectrics. The final film consists of monodisperse gold NCs arranged within a silica or organosilsesquioxane host matrix in an fcc mesostructure with precisely controlled interparticle spacings.

## 2. Results and Discussion

Scheme 1 shows the schematic synthetic processes of such ordered superlattice thin films. Water-soluble gold NC micelles were prepared by an interfacially driven microemulsion process<sup>[19,29,31]</sup> using cetyltrimethyl ammonium bromide (CTAB) and *n*-dodecanethiol (*n*-DT)-derivatized gold NCs. *n*-DT-capped gold NCs were prepared according to the method of Brust et al.<sup>[34]</sup> followed by heat treatment to narrow the gold NC size distribution to approximately 7% (see Scheme 1, step i).<sup>[35]</sup> The thermodynamically favorable interdigitation between the *n*-DT and CTAB layers stabilizes the gold NC micelles in aqueous solution.<sup>[30]</sup> Tetraethylorthosilicate (TEOS) was used as a precursor and was added to the above solution, followed by hydrolysis and condensation under acidic conditions at room temperature for 1 h. In addition to TEOS, bis(triethoxysilyl) ethane (BTEE) was used to tune the matrix composition within the superlattice films. Ordered superlattice thin films were prepared by spin-coating the above solution on substrates such as silicon wafers, glass, etc. (see Scheme 1, step ii). In order to study the siloxane condensation effect on the formation of an ordered superlattice, the above solution was aged at room temperature for different periods of time before spin-coating.

The gold/silica superlattice films have an average refractive index of ca. 1.7 and thicknesses of 100 to 300 nm depending on the spin rate. The film thickness can reach up to 25 μm when casting. Figure 1D shows an optical microscopy image of a red-



**Scheme 1.** Formation of water-soluble gold-NC micelles by surfactant/lipid encapsulation (i) and their self-assembly with soluble silica in a controlled sol-gel process (ii) into ordered gold NC/silica superlattice films through spin coating (iii); A) *n*-Dodecanethiol (*n*-DT)-stabilized, hydrophobic gold NCs; B) *n*-DT-stabilized gold NCs are encapsulated inside surfactant micelles by an interfacially driven oil-in-water microemulsion process [19]. C) Sol-gel self-assembly is conducted in acidic conditions; water-soluble oligomeric silica species preferentially interact with gold NC micelles and further self-assemble into fcc gold-NC superlattice films (D) upon drying (iii).

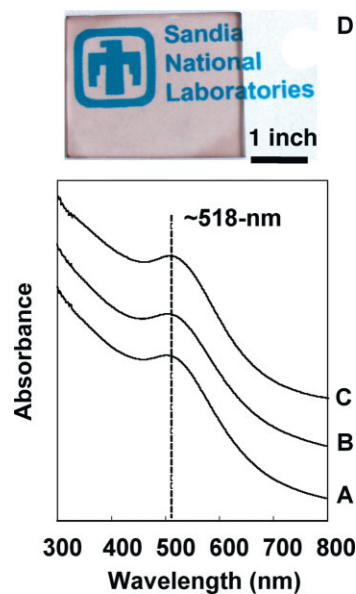


**Figure 1.** UV-vis spectra of A) *n*-DT-stabilized gold NCs, B) a gold-NC/silica superlattice film prepared using TEOS, and C) gold/ethyl bridged silsesquioxane film prepared using bis(triethoxysilyl) ethane. D) Optical microscopy image of as-prepared ordered gold/silica film on a glass substrate that covers the logo of Sandia National Laboratories (1 in = 2.54 cm).

dish film that exhibits very good optical transparency. Optical properties of the superlattice film were characterized using UV-vis spectroscopy, as shown in Figures 1A–C. The superlattice film exhibits a characteristic surface plasmon resonance band at ca. 518 nm, as expected from gold NCs. In comparison with the spectra of monodisperse *n*-DT-stabilized gold NCs, the position and width of the surface plasmon band from the gold superlattice film stays unchanged, suggesting that gold NCs inside the film remain monodisperse. This was further confirmed by TEM results (see below). Low-magnification scanning electron microscopy (SEM) imaging (Fig. 2A) shows that the film has a uniform and continuous surface without macroscopic granularity or cracks. Figure 2B shows a high-res-

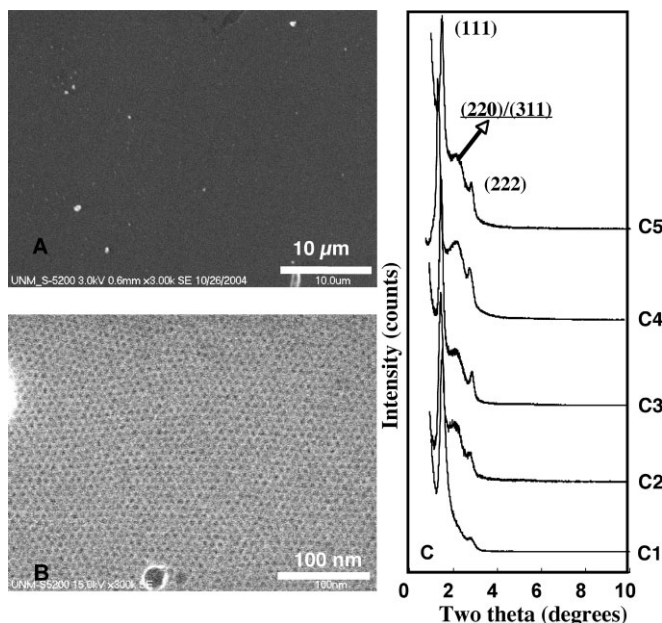


**Figure 2.** A) Low-resolution SEM image of ordered gold NC/silica superlattice thin film. B) High-resolution SEM image from the same specimen as in (A). C) X-ray diffraction patterns of gold NC/silica superlattice films. Ordered gold/silica film prepared using a coating solution that was aged under ambient conditions for 24 h (C1), and 5 h (C2). C3) Ordered gold/silica film prepared using a coating solution without aging. C4) Ordered gold/silsesquioxane film prepared using a solution that was aged under ambient conditions for 24 h. C5) Ordered gold/silsesquioxane film prepared using a solution without aging.

olution SEM image of the as-prepared film surface. Ordered gold NCs are distributed uniformly on the film surface.

Figure 2C3 shows a representative low-angle X-ray diffraction (XRD) pattern of a superlattice thin film prepared according to pathway i–iii (Scheme 1), using ca. 3 nm *n*-DT-stabilized gold NCs, CTAB, and TEOS. The patterns can be indexed as an fcc structure with unit cell  $a \sim 10.5$  nm. The primary peaks are assigned as (111), (220)/(311), and (222) reflections. Figure 2C1 shows the XRD pattern of a film prepared using a spin solution aged at room temperature for 24 h. The film exhibits a lower degree of ordering, with the disappearance of the (220)/(311) and an intensity decrease of the (222) reflections. Figure 3A shows a representative cross-sectional TEM image of

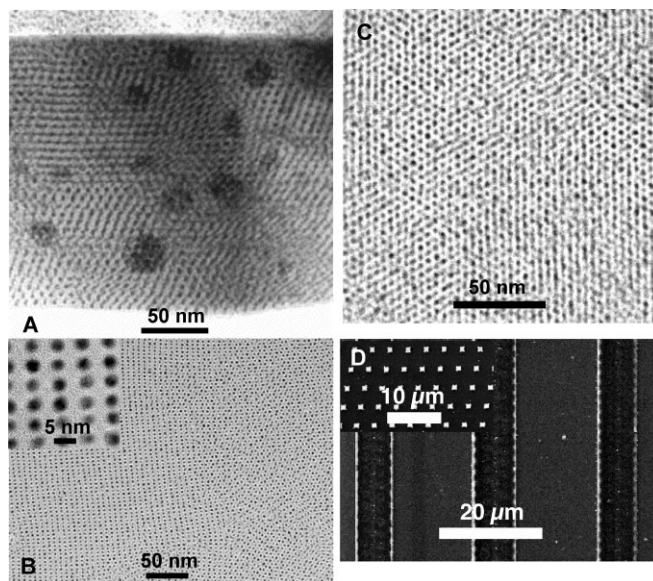


**Figure 3.** A) Cross-sectional TEM image of ordered gold NC/silica superlattice thin film. B) Representative plan-view TEM image of ordered gold NC/silica superlattice films through complete film thickness showing a seamless transition among three ordered domains [211] and [111]. Inset: a high-resolution TEM image. C) Representative plan-view TEM image of ordered gold NC/silsesquioxane superlattice films prepared using BTEE. D) Patterned gold NC/silica superlattice thin films fabricated by a micro-molding method [42]. Inset: square-dot patterns with smaller feature size.

an ordered superlattice film. Periodically ordered regions are observed throughout the whole film thickness. The sharp, continuous, and uniform air/film and film/substrate interfaces are consistent with the SEM results, showing no steps, kinks, or cracking, which appear in superlattice films prepared by evaporation of NC solutions.<sup>[14,36,37]</sup> A representative plan-view TEM image is shown in Figure 3B. The TEM images are consistent with an fcc structure ( $Fm\bar{3}m$  space group) with a measured unit cell  $a \sim 10.8$  nm and a minimum average interparticle spacing of ca. 2.3 nm. Note that the gold NC/silica superlattice thin film has a larger unit cell than that of previous superlattice films and solids.<sup>[38]</sup> This is due to the fact that here the gold NCs are arranged within a silica matrix. A thin silica layer exists between each individual gold NC. The silica insulating layer was further confirmed by a high-resolution TEM image (Fig. 3B, inset). As shown in the plan-view image (Fig. 3B), regions of ordered gold-NC arrays inside silica exhibit no preferred orientation, with a seamless transition between the ordered domains of gold NCs. Within the film, the gold NCs remain monodisperse, which is consistent with UV-vis results (see Fig. 1).

The formation of ordered gold NC/silica thin films is analogous to that of the self-assembly of surfactant and silica. Charge interactions and hydrogen bonding between hydrolyzed silica and surfactant head groups on the NC-micelle surface drive the formation of an ordered gold NC/silica mesophase.<sup>[39]</sup> However, the two systems exhibit a distinct tendency to form mesostructures. Prior work on the self-assembly of

pure surfactant and silica indicated that a series of mesostructures can be formed, including lamellar, 1D hexagonal, cubic, and 3D hexagonal periodic symmetries.<sup>[39]</sup> In the case of the self-assembly of NC micelles and silica, only fcc mesostructures are preferentially formed, regardless of the basic and acidic catalytic conditions. This is probably due to the fact that the gold NC micelles are preformed in a homogeneous solution and behave rather like a “hard” sphere, tending to form fcc close packing, rather than “soft” pure surfactant micelles, which are inclined to undergo phase transformation. Vital to the formation of transparent, ordered gold-NC/silica superlattice films is the use of stable and homogeneous spinning or casting solutions that, upon evaporation of water, undergo self-assembly of NC micelles and soluble silica. For this purpose, we prepared oligomeric silica sols in NC micelle aqueous solution with a low hydronium ion concentration (ca. pH2), which were designed to minimize the siloxane condensation rate and thereby enable facile silica and NC micelle self-assembly during spin-coating or casting.<sup>[32]</sup> The aging experiments (Fig. 2C1–3) unambiguously demonstrate that extensive silica condensation, which results in polymeric silica species, does not favor self-assembly, leading to a less-ordered film. The method is flexible, and allows the tuning of framework composition, and thus the dielectric ( $k$ ) properties, by using different sol–gel precursors. Organo-bridged silsesquioxane is an ideal, low- $k$  host, exhibiting chemical and mechanical robustness.<sup>[40,41]</sup> In addition to silica, we have demonstrated the synthesis of ordered gold-NC arrays inside an organosilsesquioxane framework. The ordered gold-NC/silsesquioxane was prepared using  $\sim 3$  nm  $n$ -DT-stabilized gold NCs, CTAB, and BTEE. The corresponding XRD patterns (Fig. 2C4,5) and TEM image (Fig. 3C) reveal that these films exhibit an ordered fcc mesostructure. In addition, we observed from the XRD results that, when using BTEE, the self-assembly is not strongly affected by solution aging, unlike the case when using TEOS. This is due to the fact that the organo-bridged precursor has a relatively slower hydrolysis and condensation rate than TEOS.<sup>[33]</sup>

The ability to form patterned films is essential for device fabrication. A homogeneous solution of gold-NC micelles allows the use of several soft-lithographic techniques, such as micro-molding, pen writing, and inkjet printing, to pattern the ordered gold-NC/silica superlattice films.<sup>[41]</sup> We have demonstrated the formation of patterned gold-NC/silica superlattice films based on our previous work on patterning surfactant-templated silica mesophases. Figure 3D shows patterned stripes and dots containing ordered gold-NC/silica superlattices fabricated using micro-molding techniques.<sup>[42]</sup> The pattern sizes are determined by the feature sizes of the poly(dimethylsiloxane) (PDMS) stamps.

In comparison to previous methods for assembling NC superlattices by the evaporation of a colloidal solution of NCs, our method provides several advantages. First, unlike previous superlattice films formed by the evaporation of organic flammable solutions, the water-soluble gold-NC micelles allow superlattice films to be fabricated in water, resulting in enhanced safety and better compatibility with current semiconductor-fabrication processing. Second, by using different sol–

gel precursors, our method allows simple tuning of framework composition, and thus dielectric properties, between the gold NCs. This is essential for achieving enhanced collective properties in such 3D superlattice films.<sup>[17,18]</sup> Furthermore, the inorganic framework provides chemical and mechanical robustness and prevents films from cracking, which is important for device fabrication. It is believed that the formation of an NC superlattice by organic solvent evaporation is an entropy-driven process in which NCs organize in such a way as to achieve the highest packing density or maximum entropy.<sup>[2,12,14,43]</sup> In our method, silica condensation affects ordering during formation of gold-NC/silica superlattice films. It is interesting to note that previous methods of assembling NCs during solvent evaporation led to two-level preferential orientations. First, the ordered NCs pack as an fcc structure with (111) planes parallel to substrates.<sup>[13,14]</sup> Second, the crystal structure of each individual NC is also orientated relative to the substrate.<sup>[13]</sup> In our system, the films consist of ordered “domains” randomly distributed throughout the film. From wide-angle XRD, we observed no preferred orientation of gold crystal structure relative to the substrate.

### 3. Conclusions

We have developed a simple and general method to synthesize ordered, 3D, transparent gold-NC/silica superlattice thin films using self-assembly of water-soluble gold NC-micelles and soluble silica by spin-coating. The self-assembly process allows the facile tuning of the host-matrix composition by using different sol–gel precursors, and provides compatibility with standard microelectronics processing/patterning, enabling higher temperature operation. Acidic sol–gel chemistry ensures spin-solution homogeneity and stability, facilitating the self-assembly of soluble silica and NC micelles into ordered, transparent gold-NC/silica films. The ease of preparing semi-conducting and magnetic NC micelles using an interfacially driven microemulsion process makes it possible to synthesize ordered quantum dot/metal oxide and magnetic NC/metal oxide arrays, and to integrate them into laser and memory devices.<sup>[30,31]</sup> The robust, 3D NC/silica superlattice films are of interest for the development of collective optical and electronic phenomena, and, importantly, for the integration of NC arrays into device architectures.<sup>[8,44]</sup> Ultimately, the ordered gold/silica superlattice films are ideal platforms for the fabrication of molecular electronic nanodevices<sup>[45]</sup> and surface-enhanced Raman spectroscopy (SERS)-based chemical and biosensors.<sup>[20,46]</sup>

### 4. Experimental

*Synthesis of Gold NCs:*  $n$ -Dodecanethiol-modified gold NCs were synthesized using the method developed by Brust et al. [34]. An aqueous solution (60 mL) containing HAuCl<sub>4</sub> (0.7 g, Aldrich) was mixed with a solution of tetraoctylammonium bromide (4 g, Aldrich) in toluene (160 mL). The two-phase mixture was vigorously stirred until the tetrachloroaurate was transferred completely into the organic layer (judged by color changes: the aqueous phase became colorless and the

organic phase became dark yellow). *n*-Dodecanethiol (0.34 g, Aldrich) was added to the organic phase. A freshly prepared aqueous solution (40 mL) of sodium borohydride (0.78 g, Aldrich) was added slowly, with vigorous stirring; the reaction was complete after 20 min. After further stirring for 2 h, the organic phase was separated and evaporated in a rotary evaporator. Heat treatment at 140 °C was performed for 30–45 min [35]. The gold NCs were then purified by two cycles of precipitation, followed by size-selective precipitation using the solvent/non-solvent pair of toluene/ethanol. In general, the gold NCs were dissolved in toluene (10 mL) and precipitated using ethanol (50 mL).

**Synthesis of Gold-NC Micelles:** In a general preparation of water-soluble gold-NC micelles, a chloroform gold-NC solution (3 mL) containing *n*-dodecanethiol-stabilized gold NCs (0.35 g) was added to deionized water (8–12 g) containing CTAB (0.2 g) under vigorous stirring, to form a solution. The chloroform was removed by quick heating to transfer the hydrophobic gold NCs into the aqueous phase by encapsulation. A dark-colored solution (stock solution) was finally obtained and centrifuged at 2000 rpm for 5 min to remove any precipitate.

**Gold NC/Silica Superlattice Thin Films:** TEOS (0.08 g) or BTEE was added to the above stock solution (1 mL), followed by the addition of aqueous HCl solution (0.07 N or 1 N, 0.05 mL). The mixture was stirred for 1 h at room temperature. Superlattice films were formed by spin-coating at 500–2000 rpm. Aging studies were performed at room temperature for the desired time.

**Characterization:** The XRD spectra were used to characterize the 3D ordered arrays (film), and were recorded on a Siemens D500 diffractometer using Ni-filtered Cu K $\alpha$  radiation with  $\lambda = 1.54 \text{ \AA}$  in  $\theta$ - $2\theta$  ( $2\theta = 1$ – $10^\circ$ ) scan mode using a step size ranging from 0.02 and a dwell time of 2 s. TEM images were taken using a JEOL 2010 high-resolution microscope equipped with a Gatan slow-scan charge-coupled device (CCD) camera and operated at 200 keV. SEM images were taken with a Hitachi S-5200 FEG high-resolution microscope.

Received: September 7, 2005

Final version: October 11, 2005

Published online: March 23, 2006

- [1] A. P. Alivisatos, *Science* **1996**, 271, 933.
- [2] M. A. El-Sayed, *Acc. Chem. Res.* **2001**, 34, 257.
- [3] B. Dubertret, P. Skourides, D. J. Norris, V. Noireaux, A. H. Brivanlou, A. Libchaber, *Science* **2002**, 298, 1759.
- [4] Y. G. Sun, Y. N. Xia, *Science* **2002**, 298, 2176.
- [5] Y. D. Yin, R. M. Rioux, C. K. Erdonmez, S. Hughes, G. A. Somorjai, A. P. Alivisatos, *Science* **2004**, 304, 711.
- [6] S. H. Sun, C. B. Murray, D. Weller, L. Folks, A. Moser, *Science* **2000**, 287, 1989.
- [7] R. P. Andres, J. D. Bielefeld, J. I. Henderson, D. B. Janes, V. R. Kola-gunta, C. P. Kubiak, W. J. Mahoney, R. G. Osifchin, *Science* **1996**, 273, 1690.
- [8] C. T. Black, C. B. Murray, R. L. Sandstrom, S. H. Sun, *Science* **2000**, 290, 1131.
- [9] C. P. Collier, R. J. Saykally, J. J. Shiang, S. E. Henrichs, J. R. Heath, *Science* **1997**, 277, 1978.
- [10] R. Doty, H. Yu, C. Shih, B. Korgel, *J. Phys. Chem. B* **2001**, 105, 8291.
- [11] M. Pileni, *J. Phys. Chem. B* **2001**, 105, 3358.
- [12] C. Murray, C. Kagan, M. Bawendi, *Annu. Rev. Mater. Sci.* **2000**, 30, 545.
- [13] C. B. Murray, C. R. Kagan, M. G. Bawendi, *Science* **1995**, 270, 1335.
- [14] M. B. Sigman, A. E. Saunders, B. A. Korgel, *Langmuir* **2004**, 20, 978.
- [15] D. V. Talapin, E. V. Shevchenko, A. Kornowski, N. Gaponik, M. Haase, A. L. Rogach, H. Weller, *Adv. Mater.* **2001**, 13, 1868.
- [16] D. V. Talapin, E. V. Shevchenko, C. B. Murray, A. Kornowski, S. Forster, H. Weller, *J. Am. Chem. Soc.* **2004**, 126, 12984.
- [17] J. Lee, V. C. Sundar, J. R. Heine, M. G. Bawendi, K. F. Jensen, *Adv. Mater.* **2000**, 12, 1102.
- [18] M. A. Petruska, A. V. Malko, P. M. Voyles, V. I. Klimov, *Adv. Mater.* **2003**, 15, 610.
- [19] H. Y. Fan, K. Yang, D. Boye, T. Sigmon, K. Malloy, H. Xu, G. P. Lopez, C. Brinker, *Science* **2004**, 304, 567.
- [20] H. Y. Fan, Y. Q. Zhou, G. P. Lopez, *Adv. Mater.* **1997**, 9, 728.
- [21] M. Epifani, C. Giannini, L. Tapfer, L. Vasanelli, *J. Am. Ceram. Soc.* **2000**, 83, 2385.
- [22] D. K. Sarkar, F. Cloutier, M. A. El Khakani, *J. Appl. Phys.* **2005**, 97, 084302.
- [23] A. Fukuoka, H. Araki, J. Kimura, Y. Sakamoto, T. Higuchi, N. Sugimoto, S. Inagaki, M. Ichikawa, *J. Mater. Chem.* **2004**, 14, 752.
- [24] Y. Guari, C. Theiuleux, A. Mehdi, C. Reye, R. J. P. Corriu, S. Gomez-Gallardo, K. Philippot, B. Chaudret, R. Dutartre, *Chem. Commun.* **2001**, 1374.
- [25] Y. Guari, C. Theiuleux, A. Mehdi, C. Reye, R. J. P. Corriu, S. Gomez-Gallardo, K. Philippot, B. Chaudret, *Chem. Mater.* **2003**, 15, 2017.
- [26] F. J. Brieler, M. Froba, L. M. Chen, P. J. Klar, W. Heimbrot, H. A. K. von Nidda, A. Loidl, *Chem. Eur. J.* **2002**, 8, 185.
- [27] A. T. Cho, J. M. Shieh, J. Shieh, Y. F. Lai, B. T. Dai, F. M. Pan, H. C. Kuo, Y. C. Lin, K. J. Chao, P. H. Liu, *Electrochem. Solid-State Lett.* **2005**, 8, G143.
- [28] H. Zeng, J. Li, J. P. Liu, Z. L. Wang, S. H. Sun, *Nature* **2002**, 420, 395.
- [29] H. Y. Fan, Z. Chen, C. Brinker, J. Clawson, T. Alam, *J. Am. Chem. Soc.* **2005**, 127, 13746.
- [30] H. Y. Fan, E. Leve, J. Gabaldon, A. Wright, R. Haddad, C. J. Brinker, *Adv. Mater.* **2005**, 17, 2587.
- [31] H. Y. Fan, E. W. Leve, C. Scullin, J. Gabaldon, D. Tallant, S. Bunge, T. Boyle, M. C. Wilson, C. J. Brinker, *Nano Lett.* **2005**, 5, 645.
- [32] C. J. Brinker, Y. F. Lu, A. Sellinger, H. Y. Fan, *Adv. Mater.* **1999**, 11, 579.
- [33] C. J. Brinker, G. W. Scherer, *Sol-Gel Science: The Physics and Chemistry of Sol-Gel Processing*, Academic Press, San Diego, CA **1990**.
- [34] M. Brust, M. Walker, D. Bethell, D. J. Schiffrin, R. Whyman, *Chem. Commun.* **1994**, 801.
- [35] M. Maye, W. Zheng, F. Leibowitz, N. Ly, C. Zhong, *Langmuir* **2000**, 16, 490.
- [36] S. Chen, *Langmuir* **2001**, 17, 2878.
- [37] C. B. Murray, C. R. Kagan, M. G. Bawendi, *Annu. Rev. Mater. Sci.* **2000**, 30, 577.
- [38] Z. L. Wang, *Adv. Mater.* **1998**, 10, 13.
- [39] Q. S. Huo, D. I. Margolese, U. Ciesla, P. Y. Feng, T. E. Gier, P. Sieger, R. Leon, P. M. Petroff, F. Schuth, G. D. Stucky, *Nature* **1994**, 368, 317.
- [40] Y. F. Lu, H. Y. Fan, N. Doke, D. A. Loy, R. A. Assink, D. A. LaVan, C. J. Brinker, *J. Am. Chem. Soc.* **2000**, 122, 5258.
- [41] H. Y. Fan, Y. F. Lu, A. Stump, S. T. Reed, T. Baer, R. Schunk, V. Perez Luna, G. P. Lopez, C. J. Brinker, *Nature* **2000**, 405, 56.
- [42] Y. N. Xia, J. A. Rogers, K. E. Paul, G. M. Whitesides, *Chem. Rev.* **1999**, 99, 1823.
- [43] B. Korgel, N. Zaccheroni, D. Fitzmaurice, *J. Am. Chem. Soc.* **1999**, 121, 3533.
- [44] A. Courty, A. Mermet, P. Albouy, E. Duval, M. Pileni, *Nat. Mater.* **2005**, 4, 395.
- [45] J. Chen, W. Wang, J. Klemic, M. A. Reed, B. W. Axelrod, D. M. Kaschak, A. M. Rawlett, D. W. Price, S. M. Dirk, J. M. Tour, D. S. Grubisha, D. W. Bennett, in *Molecular Electronics II* (Eds: A. Aviram, M. Ratner, V. Mujica), Annals of the New York Academy of Sciences, Vol. 960, New York Academy of Sciences, New York **2002**, p. 69.
- [46] Y. W. C. Cao, R. C. Jin, C. A. Mirkin, *Science* **2002**, 297, 1536.